

# MICROMECHANICAL VS LAMINA BASED FAILURE THEORIES

J. Anders Holmberg, Peter Lundmark and David Mattsson

Swerea SICOMP AB  
Box 231, SE-941 26 Piteå, Sweden  
anders.holmberg@swerea.se

## ABSTRACT

Current design practice for composite structures relies on rather simple analysis procedures and failure criteria that are supplemented by extensive testing. To deduce material and design allowables, testing is performed at the expected extremes of the service environment both at coupon and higher structural levels. Design guidelines that limit lay-up patterns and geometrical features are also employed to ensure that failure modes become fibre dominated and hence also possible to predict with reasonable accuracy.

To reduce the amount of testing and enabling more optimised designs than currently permitted, it is necessary to make use both of analysis procedures that accurately predict the actual material state at relevant micro structural scales and of a failure criterion that is using such information. Consider for instance thermal residual stresses. These develop at lamina level (meso-scale) as a consequence of the mis-match in thermal expansion between the plies in a laminate. Thermal residual stresses do however also develop at the fibre-resin level (micro-scale) due to the mis-match in thermal expansion between the constituents. All failure theories in common use are applied on the lamina or laminate level and hence all of them also neglect the influence from micro-scale residual stresses. Accounting for the micro-scale residual stresses appears however to be important when failure is to be predicted for a wide variety of loads and environments based on a limited set of experimental data.

Within this work, Strain Invariant Failure Theory (SIFT), where residual strains at all scales can be accounted for, is compared to the traditional lamina based Tsai-Hill criterion. Failure envelopes for laminas and laminates with and without including the effect of thermal residual stresses are created and compared. Comparisons are also made with experimental data from the World Wide Failure Exercise. The results suggest that lamina based criteria may consider residual stresses equally well as the micromechanical criteria at the environment where the strength parameters were determined. A review is also made of the combined SIFT and Accelerated Testing Methodology (ATM) approach for durability assessment at arbitrary environmental conditions. Several issues with the current methodology are highlighted and it is concluded that further research is needed to mature and validate the methodology before it can be safely used as an alternative to lamina based failure criteria for final design and certification purposes.

## 1. INTRODUCTION

Current design practice for composite structures relies on rather simple analysis procedures and failure criteria that are supplemented by extensive testing. To deduce material and design allowables, testing is performed at the expected extremes of the service environment both at coupon and higher structural levels. Design guidelines that limit lay-up patterns and geometrical features are also employed to ensure that failure modes become fibre dominated and hence also possible to predict with reasonable accuracy.

To reduce the amount of testing and enabling more optimised designs than currently permitted, it is necessary to make use both of analysis procedures that accurately predict the actual material state at relevant micro structural scales and of a failure criterion that is using such information. Consider for instance thermal residual stresses. These develop at lamina level (meso-scale) as a consequence of the mis-match in thermal

expansion between the plies in a laminate. Thermal residual stresses do however also develop at the fibre-resin level (micro-scale) due to the mis-match in thermal expansion between the constituents. All failure theories in common use are applied on the lamina or laminate level and hence all of them also neglect the influence from micro-scale residual stresses. Accounting for the micro-scale residual stresses appears however to be important when failure is to be predicted for a wide variety of loads and environments based on a limited set of experimental data.

The rather newly developed failure theory, Strain Invariant Failure Theory (SIFT) [1], is a fully 3D approach which includes a set of micromechanics based criteria that include the thermal residual strains also at the micro-scale. The critical effective properties of a lamina that control damage initiation are the effective volumetric and equivalent strains of the constituents, fibre and resin. The volumetric strain is the first invariant of the strain whereas the equivalent (or von Mises) strain is a function of the second invariant of the strain deviator tensor.

Within this work, SIFT is compared to the Tsai-Hill criterion, a traditional lamina based failure criteria. Failure envelopes for laminas and laminates with and without including the effect of thermal residual stresses are created and compared. Comparisons are also made with experimental data from selected cases of the World Wide Failure Exercise (WWFE). Based on these results conclusions are made regarding the feasibility for using lamina and micro-scale based failure criteria for laminates subjected to environmental loads.

## 2. STRAIN INVARIANT FAILURE THEORY

The strain invariants are defined as [1],

$$J_1 = \varepsilon_1^M + \varepsilon_2^M + \varepsilon_3^M \quad (1)$$

$$\varepsilon_{vM} = \sqrt{\frac{1}{2} [(\varepsilon_1^M - \varepsilon_2^M)^2 + (\varepsilon_1^M - \varepsilon_3^M)^2 + (\varepsilon_2^M - \varepsilon_3^M)^2] + \frac{3}{4} [\gamma_{12}^{M^2} + \gamma_{13}^{M^2} + \gamma_{23}^{M^2}]} \quad (2)$$

where  $\varepsilon_i^M$  is the local engineering strains generated by stresses (mechanical strains). 1, 2, and 3 denote the principal ply directions. The theory is usually applied to distinguish between four separate failure modes;

### Matrix resin failure by micro-cavitation

$$J_1^m \geq J_1^{m,cr} \quad (3)$$

where the superscript  $m$  denotes the matrix and  $J_1^{m,cr}$  is the critical value.

### Resin yield failure,

$$\varepsilon_{vM}^m \geq \varepsilon_{vM}^{m,cr} \quad (4)$$

where  $\varepsilon_{vM}^{m,cr}$  is the critical value for resin failure by yielding.

### Fibre failure by yielding,

$$\varepsilon_{vM}^f \geq \varepsilon_{vM}^{f,cr} \quad (5)$$

### Fibre failure by micro buckling, [2]

$$\varepsilon_{vM}^f \geq \varepsilon_{vM}^{f,cr-} \text{ if } \varepsilon_1^{fM} < 0 \quad (6)$$

The local micromechanical strains within a representative volume element (RVE) or unit cell may be determined from homogenized ply level strains using the relation,

$$\boldsymbol{\varepsilon}_i^M(\mathbf{x}) = \Lambda_{ij}(\mathbf{x})\bar{\boldsymbol{\varepsilon}}_j(\mathbf{x}_G) + (\Gamma_i(\mathbf{x}) - \alpha_i(\mathbf{x}))\Delta\theta(\mathbf{x}_G) \quad (7)$$

where we have made use of Voigt contracted notation.  $\bar{\boldsymbol{\varepsilon}}_j(\mathbf{x}_G)$  is the homogenized total strain vector (total ply strains) and  $\Delta\theta(\mathbf{x}_G)$  is the temperature offset from the stress free temperature at global position  $\mathbf{x}_G$ .  $\boldsymbol{\varepsilon}_i^M(\mathbf{x})$  is the local mechanical strain at position  $\mathbf{x}$  within the RVE and  $\Lambda_{ij}$  is the strain localization matrix (sometimes also referred to as strain magnification factor).  $\Gamma_i$  is a thermal strain localisation vector, identically zero at the boundaries of the RVE, that defines the mechanical strains induced by the coefficient of thermal expansion (CTE) mismatch between fibre and matrix.  $\alpha_i(\mathbf{x})$  is the CTE of the constituent at position  $\mathbf{x}$ . The strain localization matrices are determined analytically or by finite element analysis of a RVE.

For flat symmetric plates subject to in-plane normal loading, classical laminate theory may be used to determine the global strains  $\bar{\boldsymbol{\varepsilon}}_j(\mathbf{x}_G)$  according to,

$$\bar{\boldsymbol{\varepsilon}}_j(\mathbf{x}_G) = \bar{S}_{ij}(\mathbf{x}_G)\bar{\boldsymbol{\sigma}}_j(\mathbf{x}) + \bar{\alpha}_i(\mathbf{x}_G)\Delta\theta(\mathbf{x}_G) \quad (8)$$

where  $\bar{S}_{ij}(\mathbf{x}_G)$ ,  $\bar{\boldsymbol{\sigma}}_j(\mathbf{x})$  and  $\bar{\alpha}_i(\mathbf{x}_G)$  are the homogenized compliance matrix, applied tractions and homogenized coefficient of thermal expansion of the plate.

Figure 1 shows the failure envelope for a unidirectional glass fibre epoxy lamina. The envelope is created using a hexagonal unit cell at 60% fibre volume, based on data for E-glass / MY-750 from the WWFE [2]. The SIFT failure envelope is created in two different manners. One that explicitly account for manufacturing induced stresses (hence,  $\Delta\theta = -100^\circ\text{C}$  in Eqn. (7)) and one that consider manufacturing induced stresses implicitly through a different set of invariants and  $\Delta\theta = 0$ . The strengths of the material and the deduced strain invariants are reported in Table 1. It is interesting to note that the failure envelopes are almost identical whether manufacturing induced stresses are explicitly accounted for or not. It is easy to show analytically that the curves representing failure by resin microcavitation must be identical as long as the failure location (position  $\mathbf{x}$  where the first strain invariant has its maximum) remains in the same position as for the test case from which the critical invariant is determined. At the highest axial stresses the failure envelopes become different because the failure location shifts for the case with  $\Delta\theta = -100^\circ\text{C}$ . This implies that use of the SIFT without accounting for micro-scale residual stresses may be unconservative. For resin failure by shear that is governed by the von Mises equivalent strain, the failure envelopes are only coincident at the stress state at which the invariants were determined, i.e. transverse compression in this case. In the current example the difference is however very small. For the two fibre failure modes there is a difference between the failure envelopes except for the longitudinal tension and compression load cases but the difference is negligible.

The invariant for resin shear yielding was in this case determined from transverse compression data. The invariant for resin shear yielding may alternatively be determined from in-plane shear test data and in this case we then obtain a slightly different value even though the failure mode is expected to be the same. There are several plausible reasons for this that needs to be investigated in future research: i.e. experimental inaccuracies, the methodology to determine manufacturing induced mechanical strains or an inaccuracy in the failure criterion itself.

To give a reference to a better known failure criterion the Tsai-Hill failure envelope is also presented in Figure 1 together with some experimental data from Case 3 of WWFE [3]. The Tsai-Hill failure criterion predicts that a transverse tensile or compressive stress component will cause a significant reduction in the compressive load carrying capacity in the fibre direction. The SIFT criterion on the other hand suggest a much less conservative, maybe even unconservative, failure envelope in the two longitudinal compression quadrants. In the two longitudinal tensional quadrants it is a rather small difference between the criteria and both appear in reasonable agreement with experimental data (with some favour for Tsai-Hill) or slightly conservative.

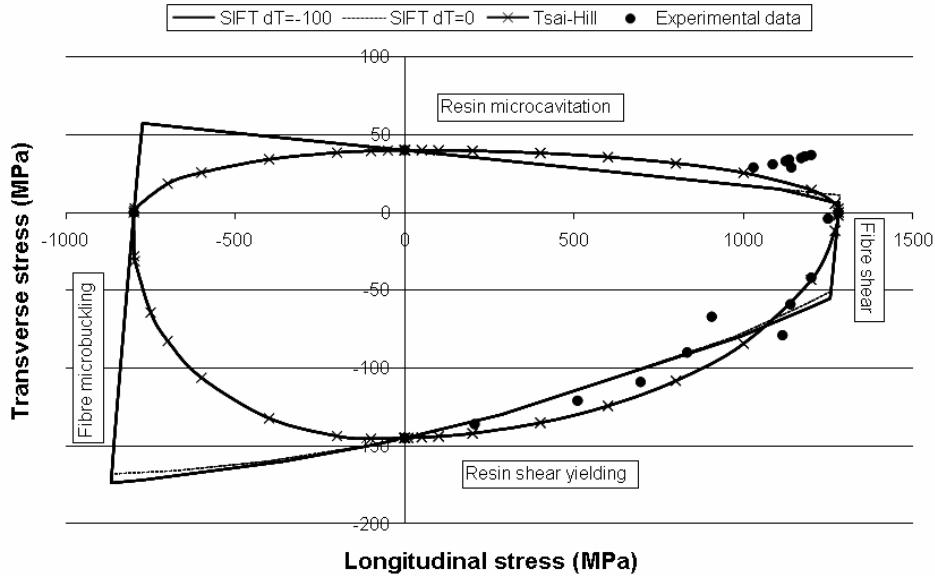


Figure 1: Lamina failure envelope according to Tsai Hill and SIFT criteria.

Table 1: Strength parameters and deduced strain invariants for E-glass / MY-750.

Loading condition	Assumed failure mode	Lamina strength	$\Delta\theta = -100^\circ\text{C}$	$\Delta\theta = 0$
			Strain invariant	Strain invariant
Longitudinal tension	Fibre shear	1280 MPa	$\epsilon_{vM+}^f = 1.94\%$	$\epsilon_{vM+}^f = 1.96\%$
Longitudinal compression	Fibre microbuckling	-800 MPa	$\epsilon_{vM-}^f = 1.25\%$	$\epsilon_{vM-}^f = 1.22\%$
Transverse tension	Resin microcavitation	40 MPa	$J_I = 2.97\%$	$J_I = 9.11\%$
Transverse compression	Resin shear yielding	-145 MPa	$\epsilon_{vM}^m = 3.60\%$	$\epsilon_{vM}^m = 2.94\%$
<i>In-plane shear</i>	<i>Resin shear yielding</i>	<i>73 MPa</i>	$\epsilon_{vM}^m = 3.13\%$	$\epsilon_{vM}^m = 3.06\%$

In Figure 2 the predicted SIFT and Tsai-Hill failure initiation envelopes of a 0/90 laminate of the same E-glass / MY-750 laminate are shown. In line with the previous discussion we present results both with and without cool-down stresses accounted for. In this case it is obvious that the residual stresses have a significant effect on the failure load. In a cross ply laminate there are residual stresses both on the homogenised ply scale, due to different thermal expansions of the  $0^\circ$  and  $90^\circ$  plies, and on the micro scale due to thermal mismatch between matrix and fibre. It appears however as if accounting for residual stresses by a linear elastic analysis of the cool-down from the cure

temperature using ambient condition material properties leads to an overestimation of the influence from the cool-down stresses. This is easier to see if we look at the predicted failure initiation strain in uniaxial tension which is reduced from 0.25% to 0.13% when cool-down stresses are accounted for (corresponding stress level is reduced from 78 to 42 MPa). Most glass fibre / epoxy laminates have a much higher failure initiation level than 0.13%. The same observation is made when studying the results of the WWFE [3], failure theories accounting for residual stresses using a linear elastic analysis were in general very conservative in their predictions of failure initiation by microcracking. Theories that did not account for residual stresses at all were on the other hand unconservative.

When comparing the SIFT and Tsai-Hill failure initiation envelopes in Figure 2 we first note that inclusion of cool-down stresses lead to a diagonal shift of the failure envelopes towards the compression-compression quadrant. The shift is almost the same for the SIFT criterion, that account for both micro scale and ply scale residual stresses, and the Tsai-Hill criterion that neglect the micro scale stresses. This implies that, at least for in-plane loading, inclusion of the micro scale residual stresses in the failure criterion do not alter the failure prediction much and hence ply level failure criteria may have sufficient precision.

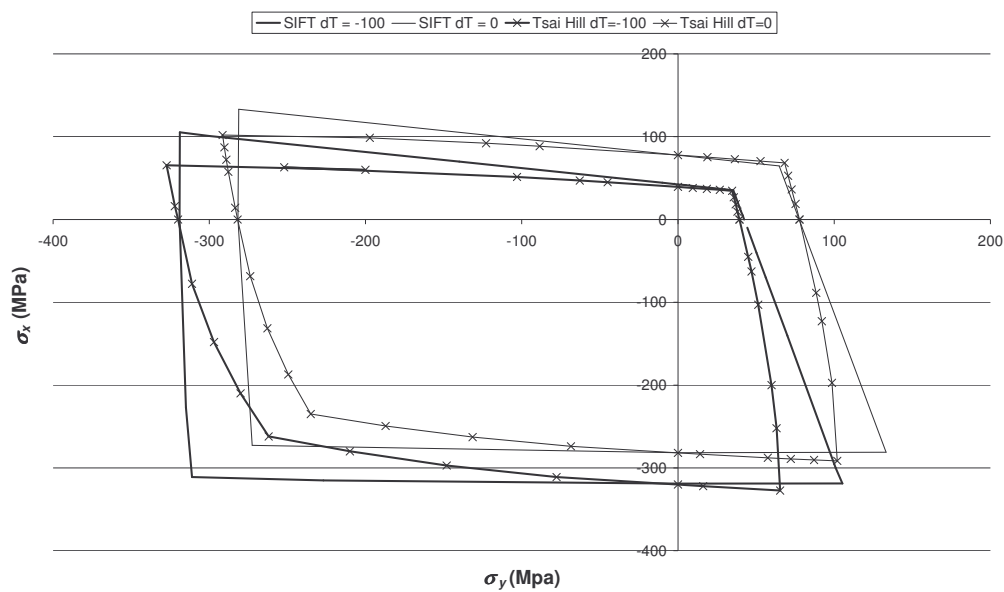


Figure 2: Failure initiation envelope of cross ply laminate according to Tsai Hill and SIFT criteria.

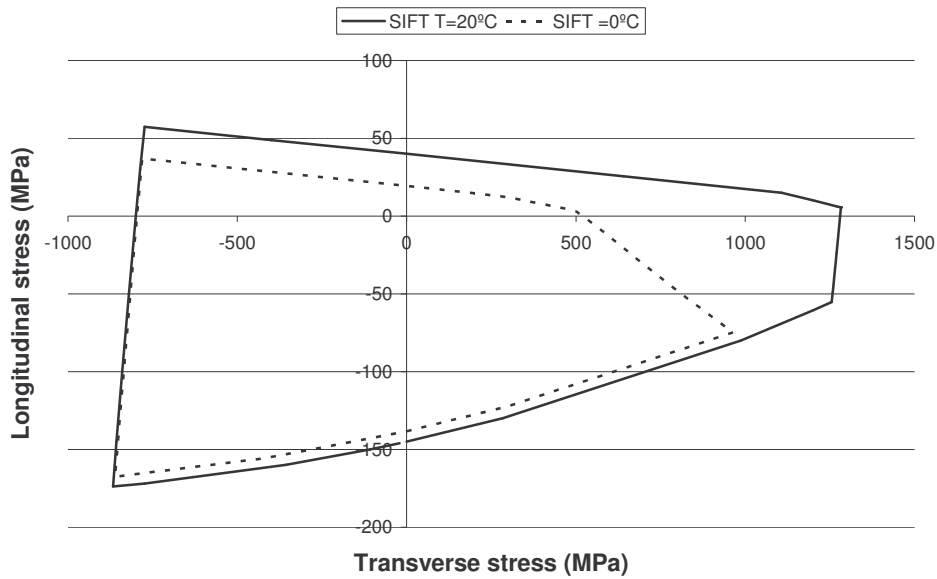


Figure 3: Lamina failure initiation envelope predicted with SIFT for ambient temperature and 0°C.

### 3. FAILURE PREDICTION AT NON-AMBIENT CONDITIONS

In order to be a practical and easy to use failure criteria, SIFT should enable prediction of failure of laminas and laminates at non-ambient conditions based only on stress analysis that include thermal and hygroscopic swelling stresses and strength parameters determined from mechanical testing at ambient conditions. Figure 3 shows how the SIFT failure initiation envelope for a lamina is predicted to change during cool-down when the strength parameters are assumed independent of the environment. There is a large reduction in the transverse tensile strength already at 0°C that is not observed in practice; normally the transverse tensile properties of unidirectional epoxy based composites are almost constant between ambient temperature and at least -50°C. It is also predicted that longitudinal splitting will precede fibre failure in longitudinal tension which also is a behaviour that is not observed in practice. For this material we actually predict that a unidirectional lamina will split without any applied mechanical loads already at -12°C which will not happen in practice. The conclusion from this exercise is that the strength parameters actually must be allowed to depend on the environment. A methodology to accomplish this while still maintaining the amount of material characterisation may be constructed by combining SIFT with the Accelerated Testing Methodology (ATM) as proposed by Kuraishi [4].

### 4. SIFT COMBINED WITH ACCELERATED TESTING METHODOLOGY

Kuraishi [4] proposed that the ATM [5] may be used to derive both the resin stiffness to be used for calculation of the strain localization factors and the critical strain invariants at specified environment and loading conditions. The theory has been implemented at Stanford University in a publicly available laminate analysis tool [6] and has been reported to give reasonable life predictions under some loading conditions, e.g. [7]. Unfortunately the methodology is only schematically described and key steps and assumptions of the analysis is not very clear. To our understanding the analysis is performed as follows (for simplicity the discussion is limited to quasi-static failure),

1. Determine critical strain invariants for the loading condition (equal load duration) and environment of interest.
  - a) Calculate critical strain invariants  $J_1^{cr}(T_{test}, t_{fail})$  and  $\epsilon_{vM}^{cr}(T_{test}, t_{fail})$  based on coupon test data.  $T_{test}$  is the test temperature and  $t_{fail}$  is the time to failure. Perform tests at a large range of loading rates and temperatures to create ATM master curves at the basis temperature  $T_{ref}$ .
  - b) Characterize the visco-elastic time-temperature-moisture shift function  $a_T(T)$  for neat resin with the same basis temperature  $T_{ref}$  as for the strength master curves.
  - c) If complete material data sets are missing for the material of interest, make use of normalized quasi-static strength versus loading rate master curves for similar materials;  $f_{J1m}(t)$ ,  $f_{\epsilon vMm}(t)$ ,  $f_{\epsilon vMf+}(t)$ , and  $f_{\epsilon vMf-}(t)$ .
  - d) Use ATM master curves to calculate the critical strain invariants for the loading condition (equal load duration) and environment of interest, e.g.

$$J_1^{m,cr}(T_1, t_1) = J_1^{m,cr}(T_{test}, t_{fail}) \cdot f_{J1m}\left(\frac{t_{fail}}{a_T(T_1)}\right) / f_{J1m}\left(\frac{t_{fail}}{a_T(T_{test})}\right) \quad (9a)$$

where  $T_1$  and  $t_1$  are the temperature and load duration of interest. If the mastercurve for the material at hand actually is available the critical invariant is determined from,

$$J_1^{m,cr}(T_1, t_1) = J_1^{m,cr}\left(T_{ref}, \frac{t_1}{a_T(T_1)}\right) \quad (9b)$$

2. Calculate strain invariants for the loading condition (equal load duration) and environment of interest.
  - a) Calculate resin relaxation modulus matrix for the loading condition (equal load duration) and environment of interest  $C_{ij}^m = C_{ij}^m(T_1, t_1)$ . The constitutive equation for the resin is approximated as,
$$\sigma_i^m(T_1, t_1) \approx C_{ij}^m(T_1, t_1) (\epsilon_j^m - \alpha_j^m(T_1 - T_0)) \quad (10)$$
where  $T_0$  refers to the stress free temperature.
  - b) Calculate 3-D ply properties and strain localization factors using micro-mechanics and the calculated resin properties.

$$\Lambda_{ij}(T, t) = g_{ij}(C_{kl}^f, C_{kl}^m(T, t), V_f) \quad (11)$$

$$\Gamma_{ij}(T, t) = h_{ij}(C_{kl}^f, C_{kl}^m(T, t), \alpha_k^f, \alpha_k^m, V_f) \quad (12)$$

where  $g_{ij}$  and  $h_i$  are the functions that relate the mechanical and thermal strain localization factors to the constituent properties and the fibre content  $V_f$ .  $C_{ij}^f$  is the elastic stiffness matrix for the fibres and  $\alpha_k^f$  and  $\alpha_k^m$  are the fibre and matrix thermal expansion coefficients. By taking the boundary average of the stress over the RVE and inserting the constitutive equation for the linear elastic fibre and Eqn. (10) for the matrix it can be shown that [8],

$$\bar{S}_{ij}(T, t) = \frac{1}{V_{RVE}} \int_{V_{RVE}} C_{ik}(\mathbf{x}_G, T, t) \Lambda_{kj}(\mathbf{x}_G, T, t) dV \quad (13)$$

$$\bar{\alpha}_i(T, t) = \frac{\bar{S}_{ij}}{V_{RVE}} \int_{V_{RVE}} C_{jk}(\mathbf{x}_G, T, t) \alpha_k(\mathbf{x}_G) dV \quad (14)$$

- c) Perform structural analysis to determine the macroscopic strain state. To include ATM in the in-plane load case previously referred to Eqn. (8) is modified to,

$$\bar{\boldsymbol{\varepsilon}}_j(\mathbf{x}_G, t_1) = \bar{S}_{ij}(\mathbf{x}_G, T_1, t_1) \bar{\boldsymbol{\sigma}}_j(\mathbf{x}, t_1) + \bar{\boldsymbol{\alpha}}_i(\mathbf{x}_G, T_1, t_1) \cdot (T_1 - T_o(\mathbf{x}_G)) \quad (15)$$

- d) Calculate local stresses and strains from the macroscopic strain state by using the strain localization factors. The applied mechanical and thermal loads must be treated separately.

$$\boldsymbol{\varepsilon}_i^M(\mathbf{x}, t_1) = \Lambda_{ij}(\mathbf{x}, T_1, t_1) \bar{\boldsymbol{\varepsilon}}_j(\mathbf{x}_G, t_1) + (\Gamma_i(\mathbf{x}, T_1, t_1) - \boldsymbol{\alpha}_i(\mathbf{x})) \cdot (T_1 - T_o(\mathbf{x}_G)) \quad (16)$$

3. Compare calculated invariants with critical invariants at the same loading condition (equal load duration) and environment of interest for the long-term strength and life prediction.

$$J_1(\mathbf{x}, t_1) \leq J_1^{cr}(T_1, t_1) \quad (17)$$

$$\boldsymbol{\varepsilon}_{vM}(\mathbf{x}, t_1) = \boldsymbol{\varepsilon}_{vM}^{cr}(T_1, t_1) \quad (18)$$

To get a good view of for which cases the combined ATM + SIFT approach may be valid it is necessary to carefully review and state approximations and assumptions of all parts of the analysis steps 1 to 3. In the following we will highlight some issues with the proposed ATM + SIFT methodology but a complete review will be the subject of future studies.

#### 4.1. Time dependency of critical strain invariants

Test cases to determine time to failure master curves for the critical strain invariants for creep loading should involve creep rupture tests where the strain invariants are maintained constant at the expected failure location in the RVE throughout the test. This would involve carefully controlled experiments where the external loading constantly is adjusted to compensate for predicted changes in strain state at the critical location in the RVE. Current testing methodology usually involve creep testing where the stress and not the strain is maintained constant. Hence the invariants will experience a change with time during the test, a change that will cause an error of unknown magnitude in the time to failure mastercurves. Similarly, constant strain rate testing should ideally be performed as constant strain invariant rate testing. It is likely but has not been shown that current test practices give accurate results.

#### 4.2. Time and temperature dependency of strain localization factors

In a more exact analysis scheme, the strain localization factors and global stiffness matrices would be determined by a fully visco-elastic analysis, e.g. [8]. In the SIFT + ATM methodology as presented in [4] Schapery's quasi-elastic method [9], Eqn. (10), is used instead of the fully visco-elastic analysis but there is no discussion about how good this approximation is and for which load cases it may be expected to be valid. Schapery shows for example that the radial stress at a fibre resin interface due to cool-down is predicted with good accuracy using the quasi-elastic method if the cool-down is fast whereas the error become increasingly large if the cool-down is slow [9]. In general the quasi-elastic method is expected to be more accurate for step loads than for ramp loads since this is the case for the direct Laplace inversion method from which it is derived [9].



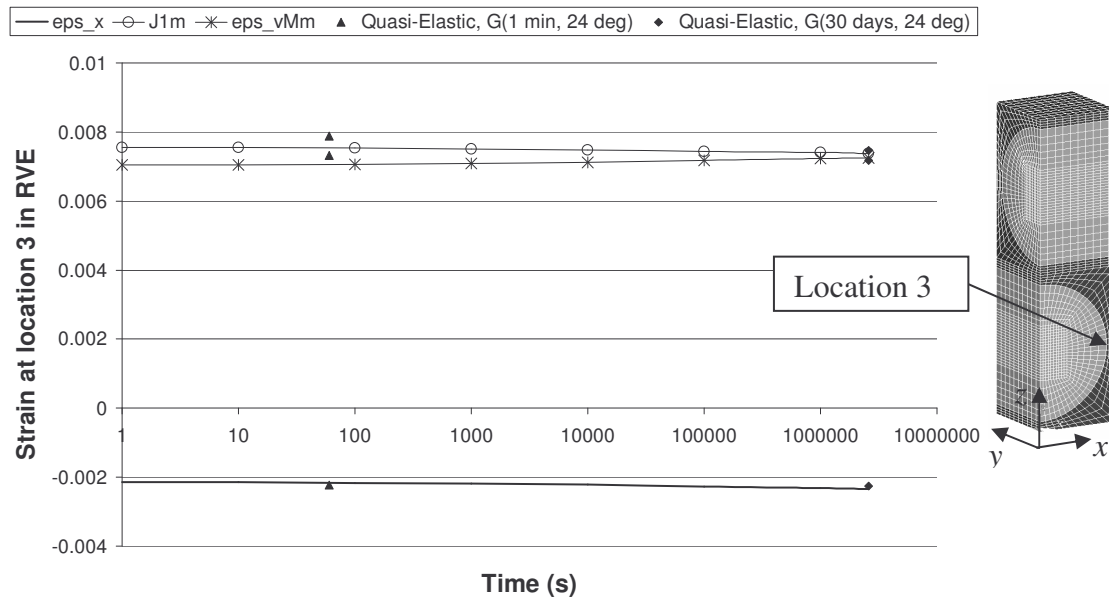


Figure 4: Variation of x-direction mechanical strain with time during ambient storage after cool-down from cure temperature.

In Figure 4 finite element simulation results for two unit cells connected to represent a  $[0/90]_s$  carbon / epoxy laminate are presented. The creep relaxation master curve and corresponding shift factor curve were extracted from Super Mic-Mac [6] for the matrix of the material type T300 / 828. Figure 4 shows the variation of local x-direction mechanical strain and the two strain invariants during ambient storage after a step cool-down from the cure temperature (as predicted using a fully visco-elastic analysis). At the times 1 minute and 1 month, corresponding results for the quasi-elastic approximation (Eqn. (10)) is presented. The data is shown for the matrix for a point that is on the fibre/matrix interface, a point where  $J_1^m$  attains it maximum when the unit-cell is mechanically loaded in the x-direction. In this case the stress relaxation is quite small and the quasi-elastic method does give a reasonable prediction of the strain state after storage even though it under predicts the strain evolution due to stress relaxation. Most likely the error will become larger if more realistic cool-down rates are considered.

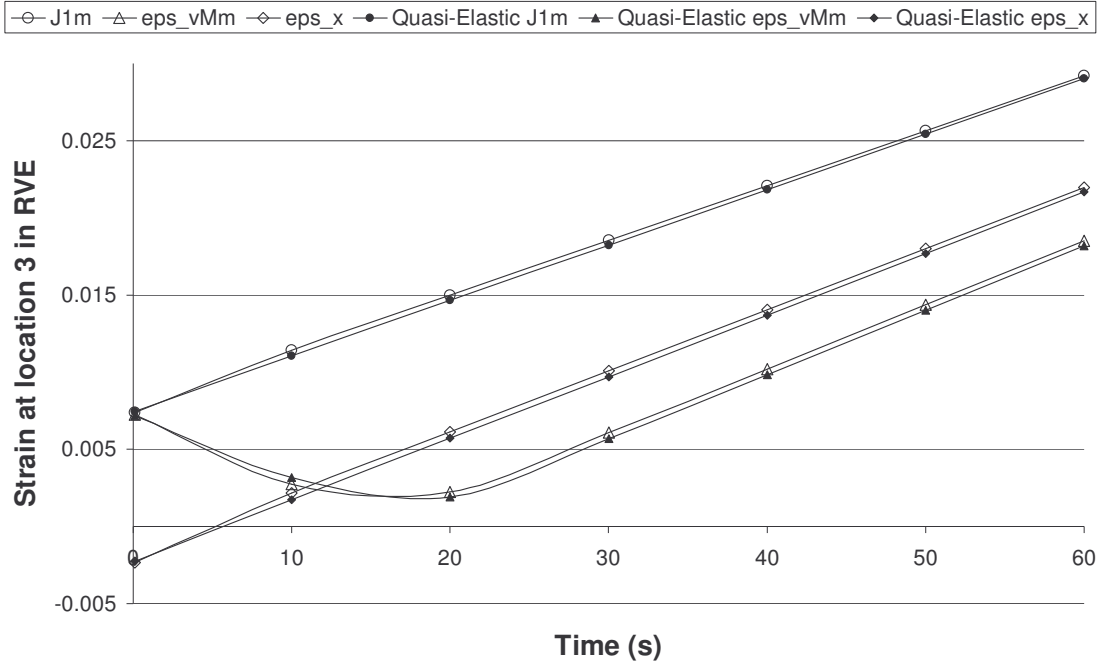


Figure 5: Variation of x-direction mechanical strain with time during constant strain rate test after 1 month ambient storage after cool-down from cure temperature.

When we add a mechanical load step after the storage time another issue become evident. Typically mechanical quasi-static testing has a duration of 1-2 minutes while the duration of the thermal loading in this example is 1 month. This means that we have two load cases with different load duration and this should be treated as two different load cases that are superposed on each other. To do this we rewrite Eqns. (10, 15 and 16) to,

$$\sigma_i^m(T_1, t_0 + t_1) \approx C_{ij}^m(T_1, t_1)(\epsilon_j^m(t_1) - \epsilon_j^m(t_0)) + C_{ij}^m(T_1, t_0 + t_1)(\epsilon_j^m(t_0) - \alpha_j^m(T_1 - T_0)) \quad (19)$$

$$\bar{\epsilon}_j^T(\mathbf{x}_G, t_0 + t_1) = \bar{\alpha}_i(\mathbf{x}_G, T_1, t_0 + t_1) \cdot (T_1 - T_0(\mathbf{x}_G)) \quad (20)$$

$$\bar{\epsilon}_j^M(\mathbf{x}_G, t_1) = \bar{S}_{ij}(\mathbf{x}_G, T_1, t_1) \bar{\sigma}_j(\mathbf{x}, t_1) \quad (21)$$

$$\begin{aligned} \epsilon_i^M(\mathbf{x}, t_0 + t_1) &= \Lambda_{ij}(\mathbf{x}, T_1, t_1) \bar{\epsilon}_j^M(\mathbf{x}_G, t_1) + \Lambda_{ij}(\mathbf{x}, T_1, t_0 + t_1) \bar{\epsilon}_j^T(\mathbf{x}_G, t_0 + t_1) \\ &+ (\Gamma_i(\mathbf{x}, T_1, t_0 + t_1) - \alpha_i(\mathbf{x})) \cdot (T_1 - T_0(\mathbf{x}_G)) \end{aligned} \quad (22)$$

where  $\bar{\epsilon}_j^T(\mathbf{x}_G, t_0 + t_1)$  is the ply strain resulting from the thermal loads due to cool-down with duration  $t_0 + t_1$  where  $t_0$  is the storage time and  $t_1$  the duration of the mechanical test.  $\bar{\epsilon}_j^M(\mathbf{x}_G, t_1)$  is the ply strain resulting from the applied mechanical load. If the mechanical test is performed at another temperature than the storage temperature the analysis procedure need to be further updated. Figure 5 present FE predicted strains in location 3 of the RVE presented in Figure 4. The RVE is subject to a constant strain rate load in the x-direction after 1 month storage at 24°C. Both results from full visco-elastic analysis and quasi-elastic analyses are presented and we see that the difference is larger than for the cool-down and storage analysis presented in Figure 4 but still rather small. The good performance of the quasi-elastic analysis in the present example is probably due to the weak visco-elastic effects at 24°C and the load durations considered. At higher temperatures or longer load durations the difference may become larger.

## 5. DISCUSSION AND CONCLUSIONS

The combined SIFT + ATM methodology has potential to enable a significant reduction of the amount of testing required at different loading and environmental conditions. The methodology appear however still rather immature and further effort is required to clearly specify the analysis procedure for general load cases, to clearly state and justify assumptions and approximations made, and to establish the precision of the methodology. Until this is accomplished the methodology will be limited to preliminary design exercises.

Lamina based failure criteria like Tsai-Hill appear to implicitly capture the influence of mechanical and environmental micro-scale stresses with reasonable accuracy provided that the lamina strength parameters are determined at the environment of interest. Also this type of failure criteria may be supported by the ATM methodology to judge the influence of environment and loading rate on the strength parameters.

## ACKNOWLEDGEMENTS

This work has been performed within a larger programme at Swerea SICOMP aimed at development and implementation of rational and accurate life assessment methodology for composite structures. The work was funded by the foundation Swedish Institute of Composites which is hereby gratefully acknowledged.

## REFERENCES

- 1- Gosse J.H., "Strain invariant failure theory for polymers in composite materials", *AIAA-2001-1184*:45-55.
- 2- Hart-Smith L.J., "Mechanistic failure criteria for carbon and glass fibers embedded in polymer matrices", *AIAA-2001-1183*:34-44.
- 3- Hinton M.J., Solden P.D., Kaddour A.S. (eds.), "Failure Criteria in Fiber-Reinforced-Polymer Composites", Special Issue *Composites Science and Technology* 2002;62:1479-1797
- 4- Hinton M.J., Solden P.D., Kaddour A.S. (eds.), "Failure Criteria in Fiber-Reinforced-Polymer Composites", Special Issue *Composites Science and Technology* 2004;64:319-588.
- 5- Kuraishi A., "Accelerated durability assessment of composite structures", *Proc. The 14th International Conference on Composite Materials*, San Diego, California; July 14–18, 2003.
- 6- Miyano Y., Kanemitsu M., Kunio T., Kuhn, H. (1986). "Role of Matrix Resin on Fracture Strengths of Unidirectional CFRP", *Journal of Composite Materials* 1986;20: 520–538.
- 7- Super Mic-Mac v2.2. <http://www.thinkcomposites.com>
- 8- Sih S., Tsai S.W., "Prediction of fatigue S-N curves of composite laminates by Super Mic-Mac", *Composites: Part A* 2005;36:1381-1388.
- 9- Allen D.H., Yoon C., "Homogenization techniques for thermoviscoelastic solids containing cracks", *International Journal of Solids and Structures* 1998;35(12):4035-4053.
- 10- Schapery R.A., "Stress analysis of viscoelastic composite materials", *Journal of Composite Materials* 1967;1:228-267.